



Resurgent regenerated fiber Bragg gratings and thermal annealing techniques for ultra-high temperature sensing beyond 1400 °C

DINUSHA SERANDI GUNAWARDENA,^{1,5} ON KIT LAW,¹ ZHENGYONG LIU,^{1,2,6}  XIAOXUAN ZHONG,³ YUK-TING HO,¹ AND HWA-YAW TAM^{1,4}

¹Photonics Research Centre, Department of Electrical Engineering, The Hong Kong Polytechnic University, Kowloon, Hong Kong SAR, China

²State Key Laboratory of Optoelectronic Materials and Technologies, School of Electronics and Information Technology, Sun Yat-sen University, Guangzhou 510275, China

³Guangdong Provincial Key Laboratory of Optical Fiber Sensing and Communications, Institute of Photonics Technology, Jinan University, Guangzhou 511443, China

⁴Photonics Research Centre, The Hong Kong Polytechnic University, Shenzhen Research Institute, Shenzhen, China

⁵dinusha.gunawardena@polyu.edu.hk

⁶liuzhengy@mail.sysu.edu.cn

Abstract: We report for the first time the resurgence of regenerated fiber Bragg gratings (RFBGs) useful for ultra-high temperature measurements exceeding 1400 °C. A detailed study of the dynamics associated with grating regeneration in six-hole microstructured optical fibers (SHMOFs) and single mode fibers (SMFs) was conducted. Rapid heating and rapid cooling techniques appeared to have a significant impact on the thermal sustainability of the RFBGs in both types of optical fibers reaching temperature regimes exceeding 1400 °C. The presence of air holes sheds new light in understanding the thermal response of RFBGs and the stresses associated with them, which governs the variation in the Bragg wavelength.

© 2020 Optical Society of America under the terms of the [OSA Open Access Publishing Agreement](#)

1. Introduction

Fiber sensors capable of measuring high temperatures are crucial for many industrial processes that require operations in harsh environments. The sensing ability of an FBG based sensor which is dependent on the peak reflectivity at a specific wavelength, experiences a severe degradation at high temperature environments restricting them from being implemented in engine turbines, power plants, steel/aluminium smelters, space exploration modules and other applications in oil and gas as well as aerospace industries where monitoring high temperature is a necessity. Over the past two decades, substantial research has been carried out to elevate the operational temperature of FBGs including hypersensitization through pre-irradiation [1], optimization of the glass composition and fabrication of type II [2] and type IIA [3] gratings using femtosecond lasers.

In the investigation of FBG sensors with improved sustainability at high temperature environments, the advent of RFBGs can be considered as a technological breakthrough which has managed to revitalize research on high-temperature sensing [4,5]. The strength of the initial seed grating (SG), pre-annealing cycle [6], fiber composition [7,8], gas loading [9], type of laser used for FBG inscription [10,11] and the applied strain [12] have been found to influence the grating regeneration process. While RFBGs have exhibited pronounced temperature stability capable of withstanding temperatures beyond 1000 °C [13], the origin and the underlying mechanisms of thermal regeneration remain controversial. Various concepts with considerable disparity have

been proposed towards explaining the formation of RFBGs. The challenge in understanding grating regeneration relies on the complex thermal processing steps and the physicochemical procedures associated with it. Although, comprehensive studies have been conducted in the investigation of the characteristics of RFBGs, majority of the reported research studies are confined to the investigation of regeneration properties in SMFs with different dopant/co-dopants whereas only a handful have demonstrated the existence of RFBGs in microstructured optical fibers (MOFs) [14]. Thus, to improve the properties of the RFBGs and their deployment in ultra-high temperature measurements, it is prudent to investigate regeneration present in various fiber structures and different regeneration techniques, which can further assist in developing a sound understanding of the grating regeneration process.

MOFs, developed through the modification of their internal structures, where most are constructed with a solid or hollow core surrounded by a periodic arrangement of air-holes running along the entire length of the fiber, play a significant role in many sensing schemes such as in pressure sensing, gas sensing, refractive index sensing and in bio sensing [15]. Suspended-core MOFs consist of relatively large air holes surrounding a small core which is suspended along the fiber length. Owing to the innate features of the suspended-core fibers, they have attracted the attention of the research community in many aspects, for instance, as bend sensors, pressure sensors, strain sensors as well as in the detection of volatile organic components (VOCs) [16]. In this study, we report for the first time to the best of our knowledge, resurgence of RFBGs referred to as resurgent regenerated fiber Bragg gratings (R²FBGs) which can sustain temperatures exceeding 1400 °C. A detailed comparison of regeneration characteristics in RFBGs present in SHMOFs and SMFs (G.657 fiber) when subjected to different thermal annealing techniques is carried out. Furthermore, the highest temperature sustainability of the two types of RFBGs and the impact on the Bragg wavelength as well as the stress changes under these annealing techniques are demonstrated as well.

2. Regeneration mechanisms

Recent studies have associated the regeneration mechanism to heat generation through UV irradiation, assisted by bond breakage, stress variations and transient excitation states induced by the laser [17]. In the investigation of glass relaxation processes, measurements of RFBGs have indicated a depression in the core and inner-cladding areas revealing an increase in density or relaxation of stresses in the interface [18]. Furthermore, micro-Raman spectroscopy has managed to reveal the difference in the local glass relaxation in the UV exposed regions, even though, annealing is similar in all areas, suggesting that the grating inscription has altered the thermal history of glass [19]. Additionally, another study has demonstrated grating regeneration in an etched fiber, signifying that grating regeneration is not entirely dependent on the structural reactions occurring at the core-cladding boundary [20]. Moreover, a diffusion-reaction mechanism based on molecular water and hydroxyl species in silica glass has also been proposed to explain the basis of RFBGs highlighting the structural changes induced by the chemical interaction and diffusion of hydrogen molecules in the glass matrix [6].

Since vitreous silica can crystallize at high temperature and pressure conditions, a model of crystallization has been proposed as well to explain grating regeneration [21]. It is assumed that formation of the crystalline polymorph cristobalite, which has a slightly higher density than vitreous silica, occurs during the process. Modification of the thermal stress in the fiber core through manipulation of the glass transition temperature via different cooling rates appeared to have a notable impact on the thermal response of the RFBGs as well [22]. Since grating regeneration involves many complicated mechanisms of various origins, careful scrutiny of other distinct factors affecting the very concepts of stress induced densification of the fiber core, crystallization and structural changes in the glass network and atomic diffusion is still required for thorough understanding of the regeneration mechanisms.

3. Experimental procedure

The SHMOF which consists of a single constituent, with regularly arranged air-holes was fabricated in-house using the stack and draw technique. The schematic illustration of the stacked preform is shown in Fig. 1(a). The air holes have a diameter of 11 μm and a pitch size of 15 μm along with a fiber outer diameter of 125 μm [Fig. 1(b)].

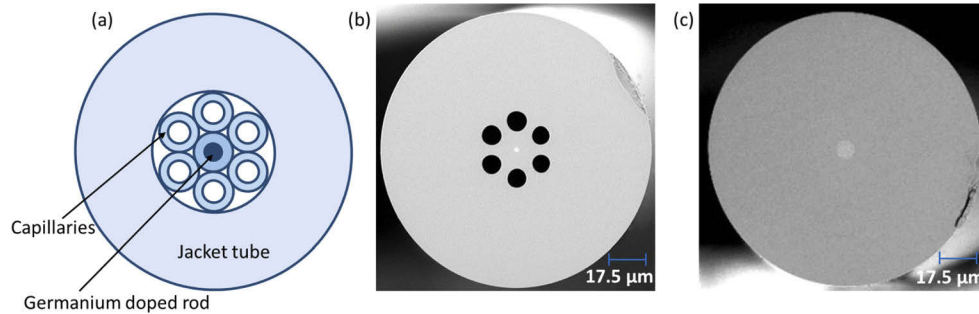


Fig. 1. (a) Schematic diagram of the stacked SHMOF preform and SEM images of (b) SHMOF and (c) SMF.

In the fiber drawing process, a vacuum pressure of ~ 40 kPa was introduced to collapse the air gaps between the rods and capillaries of the stacked preform structure. The capillaries are composed of pure silica and do not include any other additional material. The drawing temperature and tension were ~ 1960 $^{\circ}\text{C}$ and ~ 0.5 N, respectively. In order to assist modal guidance and FBG inscription, a germanium (Ge) doped region (~ 4 mol%) with a diameter of ~ 2 μm was introduced to the SHMOF. The NA of the fiber is 0.114. Subsequently, with the aid of 193 nm ArF excimer laser and a phasemask with a pitch of 1072.2 nm, FBGs were inscribed in the SHMOFs and SMFs [Fig. 1(c)]. Prior to the grating inscription procedure, all the fibers were loaded in a H_2 chamber at a pressure of 1500 Psi for two weeks. 10 mm long gratings with a Bragg transmission depth of ~ 25 dB were inscribed via pulsed UV irradiation in these fibers with a pulse energy of 80 mJ and 15 Hz repetition rate. Following FBG inscription, the FBGs were annealed at 80 $^{\circ}\text{C}$ for 12 hours to remove any residual H_2 . A commercial fusion splicer (FITEL-S178) was used to connect the SHMOFs with SMF using a manual splicing process. The similar outer diameters of SMF and SHMOF permit the cladding boundaries to be manually aligned and then spliced under reduced arc strength. Afterwards, the FBGs were inserted one at a time to a muffle furnace (SG-XS 1700) with a maximum operational temperature of 1600 $^{\circ}\text{C}$ and were subjected to various thermal annealing cycles. Firstly, the regeneration characteristics of the two types of fibers were investigated and subsequently, the fibers underwent rapid heating and rapid cooling techniques which are described in detail in the forthcoming sections.

4. Resurgence of regenerated fiber Bragg gratings

4.1. RFBGs in SHMOF and SMF

The fabrication of RFBGs are based on the thermal treatment of a UV inscribed type I FBG known as the SG. Depending on the type of optical fiber, generally, when the SG is heated up to a temperature in the range of 800-1000 $^{\circ}\text{C}$, an erasure of the SG occurs and leads to the formation of a high temperature resistant grating referred to as an RFBG. In the investigation of regeneration characteristics of gratings inscribed in SHMOF and SMF, the FBGs were placed inside a dry silica capillary tube which was in turn placed inside a muffle furnace one at a time and the temperature was ramped at 3 $^{\circ}\text{C}/\text{min}$ up to their regeneration temperatures which are 900 $^{\circ}\text{C}$ and 925 $^{\circ}\text{C}$ for SHMOF and SMF, respectively. At this point, the SGs completely disappear

and the appearance of RFBGs is observed. The temperatures were dwelled for 60 min until the completion of the grating regeneration process where the reflected peak power of each RFBG was completely stabilized. The reflection spectra were monitored using an interrogator (Micron Optics: si155) and recorded using a LabVIEW program throughout the experiment. Afterwards, the samples were naturally cooled down to room temperature inside the furnace. Figure 2(a) shows the evolution of the grating reflectivity and the shift of the Bragg wavelength, λ_B of FBGs in SHMOF and SMF, respectively. With rising temperature, the SG of SHMOF gradually decays due to the decrease in the UV induced index modulation until a complete erasure occurs at 900 °C where the RFBG emerges and stabilizes. For SMF, this phenomenon is observed at 925 °C. When the peak power of the SGs and the RFBGs are taken into consideration, evidently, a higher ratio is observed for SMF compared to that of SHMOF signifying a higher index modulation ratio, $\Delta n_{\text{reg}}/\Delta n_{\text{seed}}$ for SMF.

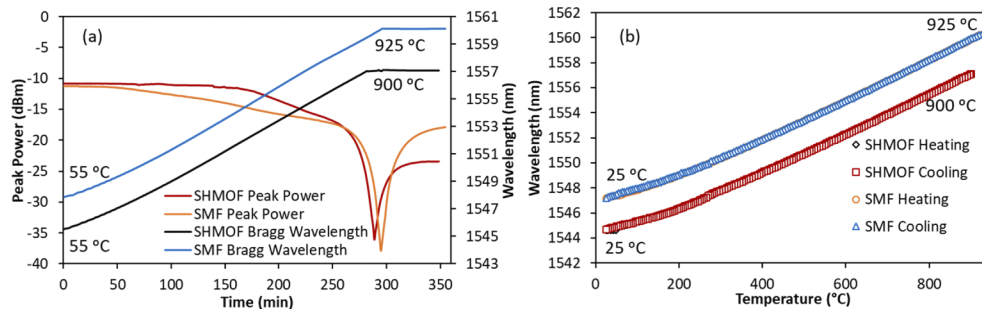


Fig. 2. (a) Evolution of the grating reflectivity and Bragg wavelength shift during thermal regeneration and (b) Heating and cooling cycles of the RFBGs in SHMOF and SMF.

In the SG, the local refractive index modulation and the density are altered during FBG inscription. Any subsequent annealing results in a structural relaxation. 193 nm UV irradiation has resulted in an increase in stress in the core-cladding interface from 100 MPa leading towards pressures over 250 MPa [23]. A variation in the stress profile exist at the core cladding interface which arises due to the thermal expansion mismatch of the constituent materials and the stresses generated during fiber drawing. Heating the fiber with CO₂ laser can reduce these stresses [1]. Although, the high index of the core appears to anneal out with rising temperature, considerable differences still exist in the glass network which dictate the final relaxation after further annealing at high temperatures. Since the presence of OH is capable of resulting in a non-exponential glass relaxation even in pure silica [24], existence of H₂ intricates the grating regeneration process. Recent discoveries of ultra-high temperature measurements on a fused silica fiber have revealed that crystallization occurs after two annealing treatments [25]. With increasing temperature, fused silica transforms into an intermediate unstable phase of α -cristobalite, and upon further heating, results in the formation of β -cristobalite. Furthermore, since vitreous silica can crystallize at high temperature and pressure conditions, pressures arising from the variation in the thermal expansion coefficient between the core and cladding which is further enhanced by the UV-induced stress during grating inscription, tends to increase the pressure within the optical fiber at these high temperatures which will influence crystallization [21]. Therefore, formation of cristobalites may very well be the structural changes that occur in RFBGs and R²FBGs which will be further discussed in the forthcoming section.

The temperature sensitivities of the RFBGs in SHMOF and SMF were characterized by conducting heating and cooling cycles as illustrated in Fig. 2(b). Overall wavelength shifts of 12.5 nm and 13.2 nm can be observed for SHMOF and SMF, respectively. When heated from ambient temperature to the maximum temperature, λ_B red shifts linearly agreeing with the Bragg condition ($\lambda_B = 2n_{\text{eff}}\Lambda$), in which both the period of the FBG, Λ (thermal expansion) and the

effective refractive index, n_{eff} (thermo-optic effect) of the fiber core rely on the temperature. Since the thermo-optic effect dominates the thermal expansion, generally, 90% of the wavelength shifts are ascribed to the variation in the refractive index of the fiber core [26]. The similar sensitivities during the heating and cooling cycles for the RFBGs in both types of fibers with the absence of any hysteresis indicate a stable response which leads towards a good sensing performance. A temperature sensitivity of 13.5 pm/°C and 14 pm/°C with an R^2 value of 99.9% were obtained for SHMOF and SMF, respectively. Figure 3(a) verifies the repeatability of the sensing characteristics of the RFBGs in both types of fibers where three heating cycles were carried out from 250 °C until the regeneration temperature of each RFBG. A complete overlap of the three heating cycles is clearly observed for the RFBGs. In order to validate the practical usage of the RFBGs and to relax the residual stress in the optical fibers, a wavelength stability test was conducted at 900 °C and 925 °C for a duration of 6.5 h for RFBGs in SHMOF and SMF, respectively and the obtained results are demonstrated in Figs. 3(b) and (c). A total wavelength drift of 0.1 nm and 0.07 nm are observed for SHMOF and SMF, respectively.

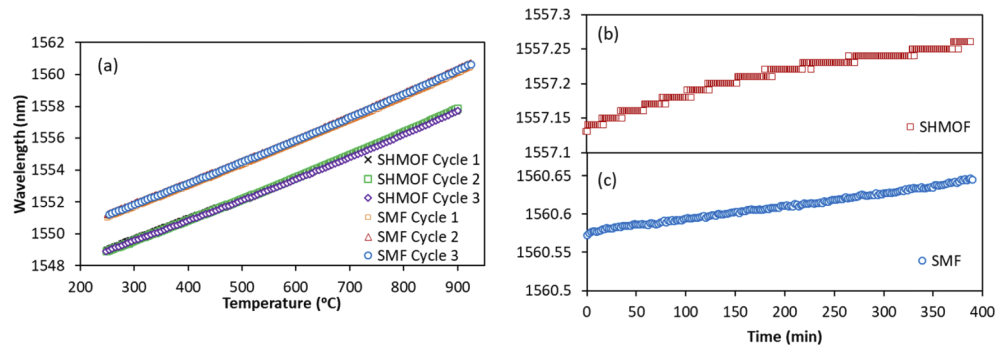


Fig. 3. (a) Temperature sensitivity calibration for three heating cycles and (b) wavelength stability of RFBGs in SHMOF and (c) SMF for 6.5 h.

4.2. R^2 FBGs in SHMOF and SMF

Further heat treatments were carried out on the RFBGs in an attempt to explore their maximum temperature sustainability. The RFBGs which underwent the annealing processes discussed in section 4.1, were further heated at a continuous ramping rate of 3 °C/min until the RFBGs were completely extinguished. Figure 4(a) illustrates the response of the peak power and the shift of λ_B of the RFBGs in SHMOF. A stable response of the peak power is observed for the RFBG until 1000 °C followed by a gradual decay of only ~3 dB until 1280 °C. At this point, the peak power starts to plummet and the RFBG gets completely submerged in background noise at 1363 °C. Furthermore, nonlinearity in the wavelength response can also be observed beyond 1280 °C. Experiments have verified that even though, the softening temperature of fused silica is ~1600 °C, silica optical fibers undergo a phase transformation leading towards the creation of microcrystals at ~1100 °C [25]. This in turn results in a transmission loss due to the devitrification of the fiber core or stress induced losses resulting from the crystal formation on the fiber surface restricting the long-term operation of fiber sensors beyond 1200 °C.

When the temperature is further increased, the resurgence of a new grating is observed which reaches a maximum peak power around 1405 °C. Afterwards, this newly created R^2 FBG was naturally cooled down to room temperature. Although, the origin of the R^2 FBG is still unclear, we believe that structural rearrangements and transformations which occur in the glass matrix together with the global change in the stresses in the fiber are responsible for this phenomenon. The cristobalite structure suspected to be formed during grating regeneration [21] consists of

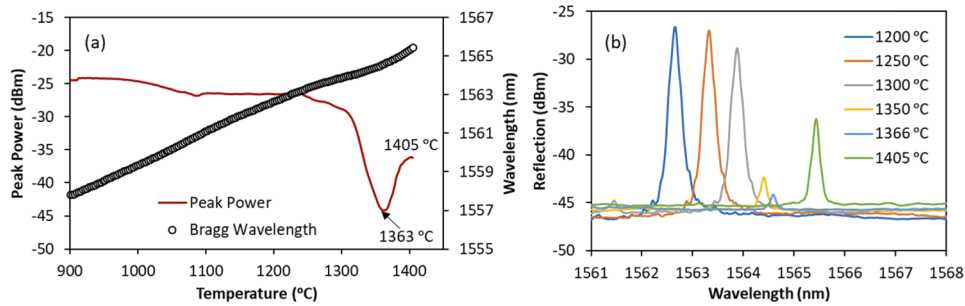


Fig. 4. (a) Peak power, wavelength shift and (b) reflection spectra of an RFBG/R²FBG in SHMOF with increasing temperature.

two varieties, namely, α -cristobalite and β -cristobalite [27]. They are crystalline polymorphs of silica and their formation at high temperatures is not directly dependent on the core dopants of the optical fiber but rather on the high temperature and high pressure [21]. Cristobalites can nucleate heterogeneously and grow internally in vitreous silica [27]. β -cristobalite is more stable than α -cristobalite at high temperatures and hence, it is possible that formation of β -cristobalite occurs and coexist with α -cristobalite post grating regeneration which explains the outstanding thermal stability of RFBGs. β -cristobalite is stable in the high temperature regimes and can be transformed back to stabilized α -cristobalite around 269 °C during the cooling down process to room temperature [25]. The growth rates of β -cristobalite in fused quartz at 1347 °C and 1408 °C are determined to be 6.5×10^{-4} $\mu\text{m}/\text{min}$ and 3.7×10^{-3} $\mu\text{m}/\text{min}$, respectively [27]. Therefore, at temperatures beyond the resurgence of RFBGs (>1363 °C), an increasingly high population of β -cristobalite exist.

Figure 4(b) shows the reflection spectra of the RFBG and the R²FBG at various temperatures throughout the heating process. Figure 5 indicates the reflection spectra of the SG, RFBG and the R²FBG in an SHMOF at room temperature (25 °C). A significant decrease in the bandwidth, side lobes and the reflected peak power is observed for the RFBGs and R²FBGs compared to that of the initial SGs. A blue shift of ~ 0.8 nm and ~ 1.25 nm in λ_B is noticed for the RFBG and R²FBG when compared to that of the SG in SHMOF. The blue shift in the RFBG compared to its SG can be ascribed to the relaxation of UV-induced Δn_{DC} [14]. Since the stress that exists in the glass structure plays a key role in determining the shift of λ_B , the further blue shift in λ_B of the R²FBG may possibly be due to the further residual stress relaxation in the glass matrix during annealing at high temperatures. The temperature sensitivity of the R²FBG was calibrated as shown in the inset of Fig. 5. A temperature sensitivity of 13.7 pm/°C was obtained over the temperature range from 250 °C to 900 °C with an R² value of 99.9% which is similar to the temperature sensitivity of its RFBG. However, in the range from 900 °C to 1370 °C a temperature sensitivity value of 15.3 pm/°C was obtained with an R² value of 99.9% and is much higher than that in the lower temperature range.

An additional heat test was carried out on another R²FBG to investigate its maximum sustainable temperature. From Fig. 6(a), it is noticed that the R²FBG in SHMOF emerges at 1407 °C and completely decays by 1452 °C denoting a maximum withstanding temperature of ~ 1450 °C. Structural modifications in the glass matrix together with the net variation in the stresses present in the core-cladding interface which is influenced by the air holes at extreme temperatures are responsible for the formation of R²FBGs in SHMOFs. The deviation of the temperature at which the resurgence of the R²FBG occurs when compared to that of Fig. 4(a), maybe due to the surface contaminants such as cladding residues which affect the formation of the cristobalite crystals [25]. Although, each sample was subjected to similar thermal treatments, and cleaned thoroughly before conducting the experiments, when a number of thermal processing

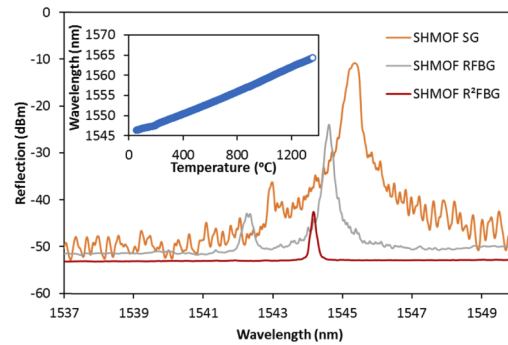


Fig. 5. Spectral profile of the SG, RFBG and R²FBG in SHMOF. The inset shows the temperature sensitivity calibration of the R²FBG.

steps are involved, it is possible for slight variations to occur which ultimately may affect the resurgent temperature of the R²FBG. Since the strength of the SG governs the strength of the RFBG [17], this concept can also be extended for the strength of the R²FBG. We believe that the weak reflectivity of the initial SG is responsible for the diminished strength of the R²FBG. Since the maximum investigated temperature reported for an RFBG to date is 1295 °C [21], this unprecedented revelation of the R²FBG which is capable of withstanding temperatures exceeding 1400 °C in an optical fiber consisting of a single constituent (Ge), is significantly important in molding the understanding of grating regeneration. Additional exploitations are still required to clarify the origin of the R²FBGs and their characteristic behavior.

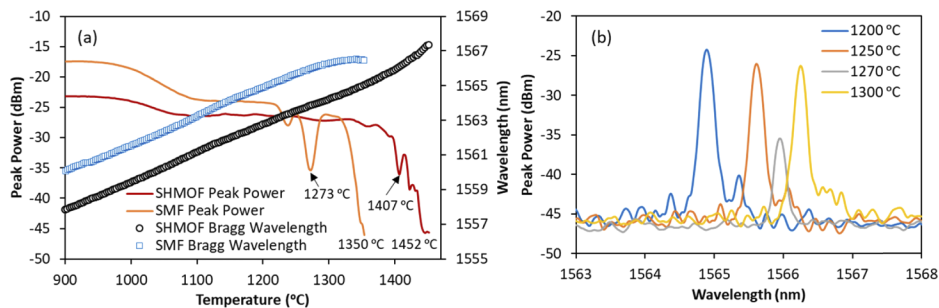


Fig. 6. (a) Peak power and wavelength shift of RFBGs in SHMOF and SMF and (b) reflection spectra of the RFBG/R²FBG in SMF with increasing temperature.

When conducting the heating process on the RFBGs in SMF, an R²FBG was observed only in a single scenario which is shown in Fig. 6(a). Figure 6(b) illustrates the reflection spectra during the heating process. The resurgence of the RFBG occurs at 1273 °C which is significantly lower to that of the two R²FBGs observed in SHMOF (1363 °C and 1407 °C) given that the regeneration temperature of the RFBG in SHMOF (900 °C) is lower than that of SMF (925 °C). However, several more investigations conducted under the same conditions failed to indicate any presence of an R²FBG in SMF, and instead led to a simple thermal decay curve of the RFBG as demonstrated in Fig. 7(a) with a highest withstanding temperature of 1387 °C. Even in the presence of an R²FBG, the highest withstanding temperature of SMF is limited to 1350 °C. Figure 7(b) indicates the reflection spectra of the SG and RFBG in SMF where an overall wavelength shift of ~0.6 nm is observed between the two. Apart from SMF, same treatment was carried out on the RFBGs in Corning SMF-28 as well. Nevertheless, any trace of an R²FBG was not observed. Hence, it is evident that in contrast to SMF, the air holes present in SHMOF

compensates the thermal stress from being transferred to the fiber core at temperatures beyond its regeneration temperature permitting the grating structure to be intact even at temperatures exceeding the resurgence of RFBGs.

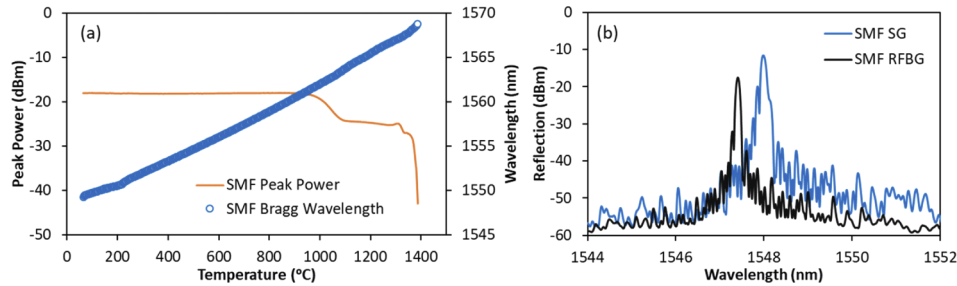


Fig. 7. (a) Peak power and wavelength shift of an RFBG in SMF with increasing temperature and (b) Spectral profile of the SG and RFBG in SMF.

5. Thermal annealing techniques and the variation of stress

In an effort to explore and enhance the performance of the RFBGs at extreme conditions, the RFBGs were exposed to two different thermal treatments.

5.1. Rapid heating

In this technique, the SGs in both types of optical fibers were inserted into a muffle furnace which was pre-heated to their respective regeneration temperatures of 900 °C (SHMOF) and 925 °C (SMF). Grating regeneration occurs in both types of fibers within 5 min as shown in Fig. 8(a). This time duration can be further reduced to seconds by subjecting the fibers to different annealing temperatures [13]. However, in this study, the intention of this approach is to investigate the maximum sustainable temperature of the RFBGs and their response to increasing temperature when exposed to extreme temperature conditions. After grating regeneration, the temperature was dwelled for 60 min for the reflected peak power of the RFBGs to completely stabilize. Figure 8(b) demonstrates the reflection spectra of the SGs and RFBGs in both SHMOF and SMF. While a blue shift in λ_B of 0.47 nm is observed for the RFBG in SHMOF compared to its SG, a negligible shift in λ_B is observed for that in SMF. Subsequently, the RFBGs in both SHMOF and SMF were further annealed to investigate their thermal decay characteristics. The thermal degradation curves of the RFBGs in SHMOF and SMF are shown in Fig. 9(a). Figures 9(b) and 9(c) show the reflection spectra of the RFBGs fabricated through the rapid heating approach with increasing temperature. The maximum withstanding temperature of the RFBGs in SHMOF and SMF amount to 1425 °C and 1200 °C, respectively. Apart from the high temperature sustainability of the RFBG in SHMOF compared to that of the RFBG in SMF, it also demonstrates a commendable spectral response even at a temperature of 1400 °C. However, in the case of SMF, the reflection spectrum initiates to split at 1050 °C and is completely distorted at 1200 °C.

This prominent enhancement of the RFBGs in SHMOF fabricated through rapid heating treatment, in terms of high temperature stability while exhibiting an admirable spectrum profile highlights the importance of the air holes in the SHMOF. When subjected to an extreme heat treatment, the air holes surrounding the fiber core in SHMOF aid in reducing the thermal stress induced to the core, thereby, permitting the RFBG to withstand elevated temperatures. Nevertheless, in SMF the thermal stress induced to the fiber core is significantly higher which in turn impacts the stability and the spectral profile of the RFBG under this extreme condition. Since the RFBG in SHMOF can clearly withstand temperatures exceeding 1400 °C when rapidly

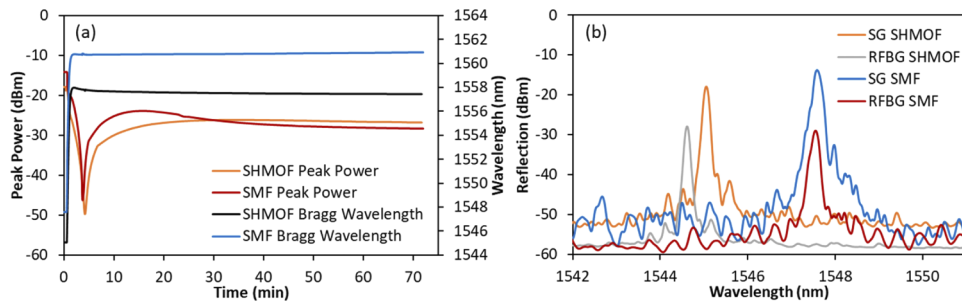


Fig. 8. (a) Evolution of the grating reflectivity and Bragg wavelength shift during thermal regeneration of rapidly heated SGs and (b) reflection spectra of the SGs and RFBGs in SHMOF and SMF.

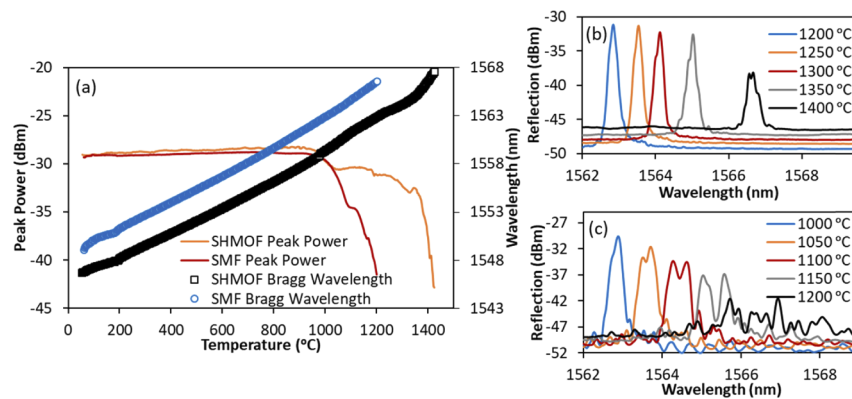


Fig. 9. (a) Thermal decay characteristics and (b) the reflection spectra of the RFBGs in SHMOF and (c) SMF with increasing temperature.

heated, its sustainability at 1350 °C was investigated and is shown in Fig. 10. The RFBG is able to successfully function for 75 min before decaying to a peak power that is undetectable by the interrogator.

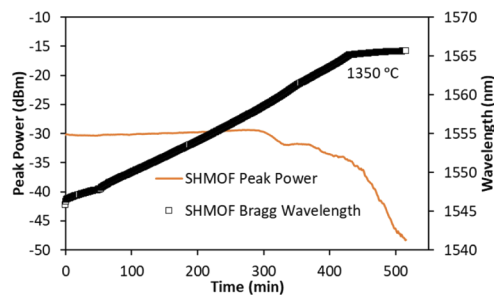


Fig. 10. Temperature sustainability of the RFBGs in SHMOF at 1350 °C fabricated through rapid heating.

5.2. Rapid cooling

In this technique, the RFBGs were fabricated as discussed in Section 4.1 and after annealing the RFBGs in both SHMOF and SMF at their respective regeneration temperatures for 6.5

h to achieve residual stress relaxation, they were instantly removed from the muffle furnace within a second. Annealing for 6.5 h reduces the residual stress in the fiber and the subsequent immediate air quenching treatment introduces compressive stress to the RFBGs. A high cooling rate is capable of inducing a large stress at the glass surface and will aid in resisting the high temperature the optical fiber experiences afterwards, resulting in a high temperature sustainability [28]. Figure 11(a) demonstrates the wavelength shift of the RFBGs in SHMOF and SMF under the rapid cooling condition and Fig. 11(b) illustrates the reflection spectra of the RFBGs in both types of optical fibers before and after the rapid cooling treatment. Red shifts in λ_B of ~ 0.2 nm and ~ 0.1 nm are observed for the RFBGs in SHMOF and SMF, respectively which underwent the treatment. Afterwards, the RFBGs were subjected to further annealing treatments to explore their highest temperature stability. Figure 12(a) shows the thermal decay curves of the RFBGs in SHMOF and SMF during high temperature annealing. A stable peak power is observed for the RFBG in SHMOF until 1305 °C followed by a gradual decrease until 1360 °C before plummeting to the noise level by 1419 °C. The reflection spectra of the RFBGs in both SHMOF and SMF with increasing temperature are shown in Figs. 12(b) and (c), respectively. For the RFBG in SMF, a stable response in the peak power is observed until 1050 °C with a gradual decay until 1350 °C before a drastic drop to the noise level by 1411 °C.

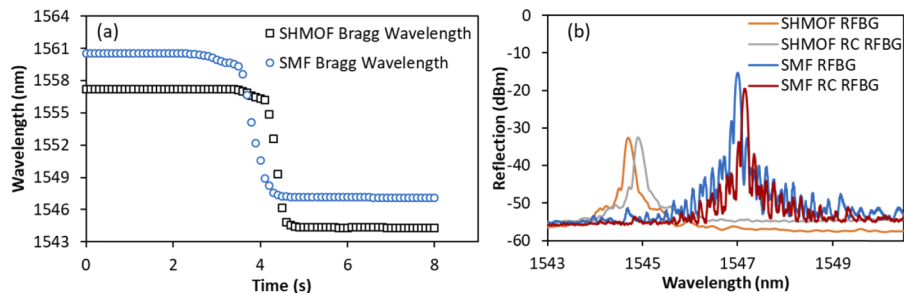


Fig. 11. (a) Wavelength response of the RFBGs in SHMOF and SMF during rapid cooling and (b) their reflection spectra at ambient temperature.

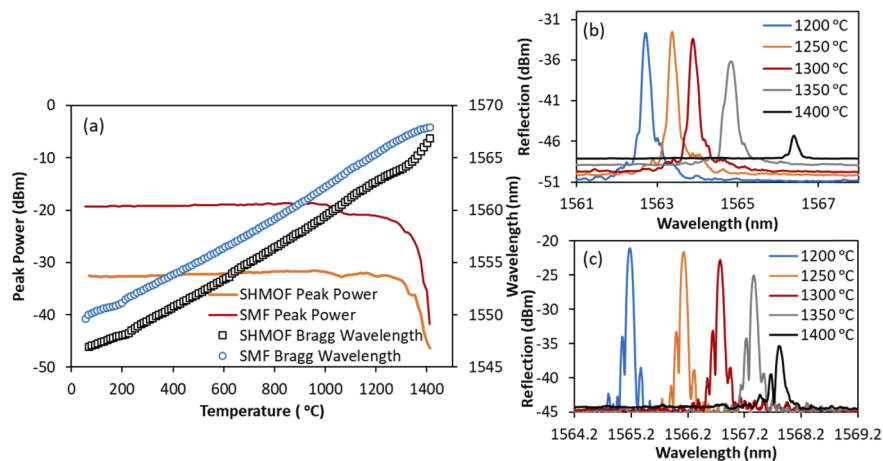


Fig. 12. (a) Thermal decay characteristics and (b) the reflection spectra of the rapidly cooled RFBGs in SHMOF and (c) SMF with increasing temperature.

Although, the RFBGs in both types of fibers appear to exhibit a similarly high temperature toleration, the thermal stability of the two RFBGs at a specific temperature reveals otherwise.

With reference to Fig. 13, it is apparent that the RFBG in SHMOF has a temperature stability which is two times higher compared to that of the RFBG in SMF at 1350 °C.

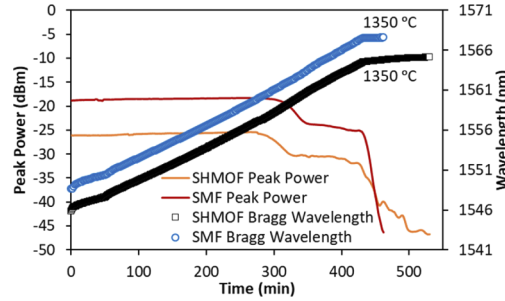


Fig. 13. Thermal stability of rapidly cooled RFBGs in SHMOF and SMF at 1350 °C.

Table 1 below summarizes the maximum sustainable temperature (T_{\max}) of the RFBGs and R²FBGs in SHMOF and SMF under general heating conditions and during rapidly heated and cooled conditions.

Table 1. Maximum temperatures of the RFBGs/R²FBGs when subjected to different thermal treatments

Type of fiber	T_{\max} of RFBG (°C)	T_{\max} of rapidly heated RFBG (°C)	T_{\max} of rapidly cooled RFBG (°C)	T_{\max} of R ² FBG (°C)
SHMOF		1425	1419	1452
SMF	1387	1200	1411	

5.3. Variation of stress

A blue shift in λ_B is observed for the RFBGs in both SHMOF and SMF compared to their SGs during the general regeneration procedure described in Section 4.1 [Figs. 5 and 7(b)]. This feature can be related to an overall increase in the tensile stress between the fiber core and cladding, as a result of the structural densification of the fiber core and the formation of the cristobalite structures during the regeneration process. Changes in the density of the fiber core affect the effective refractive index (Δn_{eff}) and the stress condition ($\Delta \sigma_z$) which can be expressed using the following equations [22,26],

$$\Delta n_{\text{eff}} = n_{\text{eff}} \left(\frac{\lambda_i}{\lambda_f} - 1 \right) \quad (1)$$

$$\Delta \sigma_z = \frac{2\Delta n_{\text{eff}}}{3C_2 + C_1} \quad (2)$$

where Δn_{eff} represents the change in the effective refractive index, n_{eff} , the effective refractive index, λ_i and λ_f , the Bragg wavelengths before and after thermal treatments at room temperature, $\Delta \sigma_z$, the change in axial thermal stress and C_1 and C_2 the stress-optic coefficients, which are $7.42 \times 10^{-12} \text{ m}^2/\text{kg}$ and $4.102 \times 10^{-11} \text{ m}^2/\text{kg}$, respectively [2,22,26,29]. Since both types of optical fibers have a similar material composition in the fiber core with the air holes in SHMOF located in the silica cladding, the stress-optic coefficients of both SHMOF and SMF are assumed to be the same over the core cross section of the fiber. Moreover, the Bragg wavelength shifts are ascribed to the variation in the refractive index of the fiber core, since the thermo-optic effect dominates over the thermal expansion effect [26]. Based on Eqs. (1) and (2), the first four bars in Fig. 14 summarize the stress changes between the SGs and RFBGs in both SHMOF and SMF

under general regeneration and rapidly heated regeneration conditions. A higher change in stress is observed for SHMOF compared to that of SMF after general grating regeneration. Although, almost half the change in stress is observed for the RFBGs in SHMOF fabricated through the rapid heating procedure compared to that of the general regeneration process, ~ 12 times higher stress change is observed for these RFBGs compared to those in SMF produced during the rapid heat treatment. This considerably low stress change in the RFBG of rapidly heated SMF compared to its SG, sheds some light in understanding the thermal decay characteristics and the poor temperature sustainability of rapidly heated RFBGs [Figs. 9(a) and (c)]. The abrupt change in temperature during rapid heating, inhibits stress relaxation of the RFBGs in SMF significantly compared to those in SHMOF, in which the presence of air holes compensates for this adverse effect. The last two bars in Fig. 14 indicate the stress change experienced by the RFBGs after the rapid cooling treatment [Fig. 11(b)]. A negative stress change of $\sim 3 \times 10^6$ kg/m² and $\sim 2 \times 10^6$ kg/m² are observed for the RFBGs in SHMOF and SMF, respectively. The annealing treatment conducted prior to the rapid cooling treatment aids in residual stress relaxation and the air quenching treatment restores stress. Hence, these negative stress changes represent the overall stress changes that occur in the optical fibers.

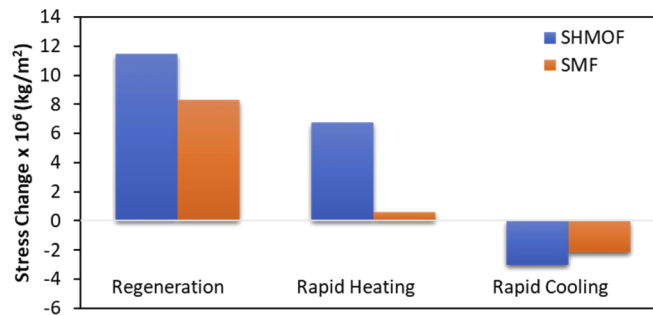


Fig. 14. Variation of stress in the fiber core of RFBGs in SHMOF and SMF after grating regeneration, rapid heating and rapid cooling tests.

In the light of the investigations, despite the thermal treatment, RFBGs in SHMOF tend to exhibit a similar thermal response although, a highest withstanding temperature with a good spectral profile is observed for the rapidly heated condition. In contrast, for the RFBGs in SMF, the best spectral response and a highest withstanding temperature is observed for the rapid cooling condition. This is a significant improvement compared to its rapidly heated condition or the general heating condition. Evidently, the air holes present in SHMOF plays a vital role in controlling and compensating the thermal stress introduced to the core of the fiber during these varying thermal treatments thereby, signifying a similar thermal response irrespective of the drastic conditions experienced by the RFBGs. Hence, these microstructured optical fibers will be excellent candidates for environments with rapid temperature fluctuations. In depth investigations on the material properties of the optical fibers are still required to understand the underlying mechanisms responsible for the resurgence of RFBGs. Therefore, material characterization using XRD and micro-Raman spectroscopy is considered as the future direction of this research study.

6. Conclusion

In this study, we have conducted a comprehensive investigation on the thermal regeneration characteristics of RFBGs in SHMOFs and SMFs and their maximum sustainable temperatures. Continuous temperature ramping in an RFBG leads to the formation of an R²FBG in both SHMOF and SMF. A highest withstanding temperature of 1450 °C and 1350 °C were observed for the R²FBGs in SHMOF and SMF, respectively. Revelation of these R²FBGs consisting of a single

constituent can lead to broadening the horizons in the development of temperature sensors for ultra-high temperature sensing. Furthermore, in an attempt to improve the maximum sustainable temperature of RFBGs, we have demonstrated the impact of two different annealing techniques on the regeneration properties of the RFBGs in both SHMOFs and SMFs. RFBGs in SHMOFs indicated a similar thermal response under these extreme conditions compared to those of SMFs emphasizing the significance of the air-hole structure in controlling and compensating the stress changes introduced when exposed to drastic temperature variations. The enhancement of the temperature sustainability of the RFBGs in SMF under the rapidly cooled condition compared to the rapidly heated condition is noteworthy as well. Moreover, the stress changes in the RFBGs of the two types of optical fibers under each treatment were determined and comparisons were made based on the obtained experimental results. The findings in this study will further contribute in understanding the origins and limitations of RFBGs in the development of ultra-high temperature sensors with optimal performance.

Funding

Hong Kong Polytechnic University (1-BBYE, 1-BBYS, 1-ZVGB); National Natural Science Foundation of China (61827820, 61905096).

References

1. M. Åslund and J. Canning, "Annealing properties of gratings written into UV-presensitized hydrogen-outdiffused optical fiber," *Opt. Lett.* **25**(10), 692–694 (2000).
2. K.-S. Lim, H.-Z. Yang, W.-Y. Chong, Y.-K. Cheong, C.-H. Lim, N. M. Ali, and H. Ahmad, "Axial contraction in etched optical fiber due to internal stress reduction," *Opt. Express* **21**(3), 2551–2562 (2013).
3. N. Grothoff and J. Canning, "Enhanced type IIA gratings for high-temperature operation," *Opt. Lett.* **29**(20), 2360–2362 (2004).
4. B. Zhang and M. Kahrizi, "High-Temperature Resistance Fiber Bragg Grating Temperature Sensor Fabrication," *IEEE Sens. J.* **7**(4), 586–591 (2007).
5. S. Bandyopadhyay, J. Canning, M. Stevenson, and K. Cook, "Ultrahigh-temperature regenerated gratings in boron-codoped germanosilicate optical fiber using 193 nm," *Opt. Lett.* **33**(16), 1917–1919 (2008).
6. P. Holmberg, F. Laurell, and M. Fokine, "Influence of pre-annealing on the thermal regeneration of fiber Bragg gratings in standard optical fibers," *Opt. Express* **23**(21), 27520–27535 (2015).
7. H. Z. Yang, X. G. Qiao, S. Das, and M. C. Paul, "Thermal regenerated grating operation at temperatures up to 1400°C using new class of multimaterial glass-based photosensitive fiber," *Opt. Lett.* **39**(22), 6438–6441 (2014).
8. D. S. Gunawardena, K. A. Mat-Sharif, M.-H. Lai, K.-S. Lim, N. Tamchek, N. Y. M. Omar, S. D. Emami, S. Z. Muhamad-Yasin, M. I. Zulkifli, Z. Yusoff, H.-Z. Yang, H. A. Abdul-Rashid, and H. Ahmad, "Thermal Activation of Regenerated Grating in Hydrogenated Gallosilicate Fiber," *IEEE Sens. J.* **16**(6), 1659–1664 (2016).
9. K. Cook, L.-Y. Shao, and J. Canning, "Regeneration and helium: regenerating Bragg gratings in helium-loaded germanosilicate optical fibre," *Opt. Mater. Express* **2**(12), 1733–1742 (2012).
10. A. Bueno, K. Chah, D. Kinet, P. Mégret, and C. Caucheteur, "Hydrogen influence on regenerated FBGs produced by the phase mask technique with 266 nm femtosecond pulses," in *Advanced Photonics Conference*, (Optical Society of America, 2014), paper. BW4D-3.
11. K. Cook, C. Smelser, J. Canning, G. le Garff, M. Lancry, and S. Mihailov, "Regenerated femtosecond fibre Bragg gratings," *Proc. SPIE* **8351**, 835111 (2012).
12. T. Wang, L.-Y. Shao, J. Canning, and K. Cook, "Regeneration of fiber Bragg gratings under strain," *Appl. Opt.* **52**(10), 2080–2085 (2013).
13. A. Bueno, D. Kinet, P. Mégret, and C. Caucheteur, "Fast thermal regeneration of fiber Bragg gratings," *Opt. Lett.* **38**(20), 4178–4181 (2013).
14. T. Chen, R. Chen, C. Jewart, B. Zhang, K. Cook, J. Canning, and K. P. Chen, "Regenerated gratings in air-hole microstructured fibers for high-temperature pressure sensing," *Opt. Lett.* **36**(18), 3542–3544 (2011).
15. A. M. R. Pinto and M. Lopez-Amo, "Photonic Crystal Fibers for Sensing Applications," *J. Sens.* **2012**, 1–21 (2012).
16. D. Lopez-Torres, A. Lopez-Aldaba, C. Elosua, J. Auguste, R. Jamier, P. Roy, M. Lopez-Amo, and F. Arregui, "Comparison between Different Structures of Suspended-Core Microstructured Optical Fibers for Volatiles Sensing," *Sensors* **18**(8), 2523 (2018).
17. J. Canning, "Regeneration, regenerated gratings and composite glass properties: the implications for high temperature micro and nano milling and optical sensing," *Measurement* **79**, 236–249 (2016).
18. M. Lancry, K. Cook, J. Cao, T. Billotte, B. Poumellec, and J. Canning, "Study of stress relaxation in UV regenerated fiber Bragg gratings," in *The European Conference on Lasers and Electro-Optics*, (Optical Society of America, 2017), paper. CM_P_25.

19. M. Lancry, K. Cook, D. Pallarés-Aldeiturriaga, J. M. Lopez-Higuera, B. Poumellec, and J. Canning, "Raman spectroscopic study of Bragg gratings regeneration," in *Advanced Photonics Conference*, (Optical Society of America, 2018), paper. BM2A-4.
20. H. Yang, W. Y. Chong, Y. K. Cheong, K.-S. Lim, C. H. Pua, S. W. Harun, and H. Ahmad, "Thermal Regeneration in Etched-Core Fiber Bragg Grating," *IEEE Sens. J.* **13**(7), 2581–2585 (2013).
21. J. Canning, M. Stevenson, S. Bandyopadhyay, and K. Cook, "Extreme silica optical fibre gratings," *Sensors* **8**(10), 6448–6452 (2008).
22. M. Lai, K. Lim, D. S. Gunawardena, H. Yang, W.-Y. Chong, and H. Ahmad, "Thermal stress modification in regenerated fiber Bragg grating via manipulation of glass transition temperature based on CO₂-laser annealing," *Opt. Lett.* **40**(5), 748–751 (2015).
23. K. W. Raine, R. Feced, S. E. Kanellopoulos, and V. A. Handerek, "Measurement of axial stress at high spatial resolution in ultraviolet-exposed fibers," *Appl. Opt.* **38**(7), 1086–1095 (1999).
24. M. Tomozawa, A. Koike, and S. R. Ryu, "Exponential structural relaxation of a high purity silica glass," *J. Non-Cryst. Solids* **354**(40-41), 4685–4690 (2008).
25. Q. Lin, N. Zhao, K. Yao, Z. Jiang, B. Tian, P. Shi, and F. Chen, "Ordinary Optical Fiber Sensor for Ultra-High Temperature Measurement Based on Infrared Radiation," *Sensors* **18**(11), 4071 (2018).
26. M. Celikin, D. Barba, B. Bastola, A. Ruediger, and F. Rosei, "Development of regenerated fiber Bragg grating sensors with long-term stability," *Opt. Express* **24**(19), 21897–21909 (2016).
27. F. E. Wagstaff, "Crystallization Kinetics of Internally Nucleated Vitreous Silica," *J. Am. Ceram. Soc.* **51**(8), 449–453 (1968).
28. Y. Li, M. Yang, C. Liao, D. Wang, J. Lu, and P. Lu, "Prestressed Fiber Bragg Grating With High Temperature Stability," *J. Lightwave Technol.* **29**(10), 1555–1559 (2011).
29. T. Martynkien, G. Statkiewicz-Barabach, J. Olszewski, J. Wojcik, P. Mergo, T. Geernaert, C. Sonnenfeld, A. Anuszkiewicz, M. K. Szczurowski, K. Tarnowski, M. Makara, K. Skorupski, J. Klimek, K. Poturaj, W. Urbanczyk, T. Nasilowski, F. Berghmans, and H. Thienpont, "Highly birefringent microstructured fibers with enhanced sensitivity to hydrostatic pressure," *Opt. Express* **18**(14), 15113–15121 (2010).